AMJ Australasian Medical Journal [AMJ 2023;16(4):585-591]

Development of a Tissue Equivalent Gelatine Phantom for Accuracy Verification of Tissue Elasticity Measurement Using Shear Wave Elastography Ultrasound

Yin How Wong[1], Huong Eng Ting[2], Kwan Hoong Ng[2], Basri Johan Jeet Abdullah[1,2], Napapong Pongnapang[3] and Chai Hong Yeong[1*]

[1]Medical Advancement for Better Quality of Life Impact Lab, and School of Medicine, Faculty of Health and Medical Sciences, Taylor's University, Selangor, Malaysia
[2]University of Malaya Research Imaging Centre and Department of Biomedical Imaging, Faculty of Medicine, University of Malaya, Kuala Lumpur, Malaysia.
[3]Department of Radiological Technology, Faculty of Medical Technology, Mahidol University, Siriraj Hospital, Bangkok, Thailand.

RESEARCH

Please cite this paper as: Wong YH, Ting HE, Ng KH, Abdullah BJJ, Pongnapang N, Yeong CH. Development of a Tissue Equivalent Gelatine Phantom for Accuracy Verification of Tissue Elasticity Measurement Using Shear Wave Elastography Ultrasound. AMJ 2023;16(4):585-591 https://doi.org/10.21767/AMJ.2022.3944

Corresponding Author:
Chai Hong Yeong,
School of Health and Medical Sciences,
Taylor's University,
Selangor, Malaysia
chaihong.yeong@taylors.edu.my

ABSTRACT

Background

Shear Wave Elastography ultrasound (SWE) has been increasingly used in the recent decade to quantify tissue stiffness and viscoelastic properties correlate to a disease condition.

Aims

This study aimed to develop a low cost and reproducible gelatine phantom to verify the accuracy of tissue elasticity measurement using (SWE). The effect of lesion's size, stiffness and depth from the surface on the tissue elasticity measurement was also investigated.

Methods

A breast tissue-equivalent phantom embedded with spherical inclusions of different sizes, stiffness and depth from surface was constructed using gelatin. The elasticity of the spherical inclusions was determined using a commercial SWE system and compared to the elasticity determined using a high precision electromechanical the offset from the SWE measurement and to account for these differences.

Results

Statistically significant difference ($p<0.05$) was found between the elasticity measured using SWE and electromechanical microtester, whereby the SWE overestimated the tissue elasticity by a mean value of 22.8 ± 15.0 kPa. The size and depth of the spherical inclusions have not imposed any effect on the elasticity measured by SWE, but the depth of shear wave detection was found limited to 8 cm from the surface.

Conclusion

The gelatine phantom constructed in this study could be used to verify the accuracy of the elasticity measured using SWE. The tissue elasticity measured by the SWE appeared to be overestimated compared to the gold standard. Further research would need to be carried out to determine the offset from the SWE measurement and to account for these differences.

Key Words

Shear wave elastography, Ultrasound, Tissue elasticity, Tissue-equivalent phantom, Instron

What this study adds:

A breast tissue-equivalent phantom was developed to verify accuracy of tissue elasticity measurement using SWE.

SWE overestimated tissue elasticity by 22.8 ± 15.0 kPa compared to the standard electromechanical microtester.

Size and depth of lesions did not affect elasticity values, but the depth of shear wave detection was limited to 8 cm from the surface.

1. What is known about this subject?

SWE is a relatively new transient elastography technique using a real-time, non-invasive and reproducible method to

map tissue stiffness.

2. What new information is offered in this study?

A cost-effective and reproducible soft tissue-equivalent gelatine phantom was developed to verify the accuracy of tissue elasticity measurement using SWE.

3. What are the implications for research, policy, or practice?

In comparison to the gold standard, the SWE system tested in this study constantly overestimated tissue elasticity by 22.8 ± 15.0 kPa.

Background

Elastography has been widely used as a non-invasive imaging tool to visualize and quantify soft tissue stiffness and viscoelastic properties. Several elastography techniques based on ultrasound and magnetic resonance have been developed to accommodate the escalating demand for clinical elastography. Clinical application of elastography relies on the changes of tissue elasticity in various pathological conditions to yield qualitative and quantitative diagnostic information[1,2,3]. Ultrasound elastography is a more popular choice over the magnetic resonance elastography due to its easier operation, wider availability and relatively lower cost of operation[4,5].

Shear Wave Ultrasound Elastography (SWE) is a relatively new transient elastography technique using a real-time, non-invasive and reproducible method to map the tissue stiffness. The tissue elasticity measurement using SWE is dependent on the velocity of the shear wave propagates in the soft tissue. The shear wave propagates slower in softer tissue but becomes faster in stiffer tissue[6]. This small difference in the velocity as the shear wave passes through the tissue of different stiffness is detected and measured at a high frame rate of up to 20,000 frames per second using the ultrafast imaging technique[7]. The tissue elasticity is then determined from the Young's modulus formula as following[8]:

$E=3\rho c^2$ Eq. 1

Where E is tissue elasticity (kPa), ρ is the local density (constant and equal to 1 g/cm^3 in soft tissue) and c is the shear wave propagation velocity.

In view of the potential of SWE to be developed as an important imaging modality in diagnostic imaging, the accuracy and reliability of the SWE for tissue elasticity estimation should be assessed. Currently, only the elasticity Quality Assurance (QA) phantoms (Model 049 and 049A) from the Computerized Imaging Reference Systems (CIRS), Inc. is commercially available as standard reference tool for determining sources of variance in shear wave elasticity measurements. The elasticity QA phantoms contain targets of known stiffness relative to the background material and range in stiffness, diameter and depth. The Model 049 is a basic QA phantom as it contains two sizes of spheres positioned at two different depths. At each depth there are two spheres that are softer than the background and two that are stiffer than the background. In view of the cost of owning the CIRS phantoms and the cost of maintenance, not all healthcare centres could own the phantoms for the accuracy validation, especially those from developing countries.

This study was taken to develop a low cost and reproducible gelatine phantom to verify the accuracy of tissue elasticity measurement using SWE. The elasticity as measured using SWE will be compared to the elasticity determined using electromechanical microtester, which is gold standard for elasticity measurement. In addition, the effect of lesion's size, stiffness and depth from the surface on the accuracy of the SWE measurement was also be investigated in this study.

Materials

Gelatine powder from lime bovine bone (LB 250) was purchased from Rousselot Gelatine Co., Ltd., Guangdong, and China. The carmoisine and calcium carbonate ($CaCO_3$) used were of analytical grade purity. The deionized water was used in all experiments.

Methods

Shear Wave Elastography Phantom

A tissue-equivalent phantom with the similar acoustic velocity (~1510 mm/s)[9] and elasticity (5 - 10 kPa, fatty tissue)[10] of human breast tissue was constructed using gelatine. Multiple spherical inclusions of different gelatine concentrations (0.05, 0.08, 0.13, 0.16 g/ml) and diameters (17, 19, 22, 26 and 30 mm) were embedded in the phantom at different depth from the surface to verify the accuracy and to investigate different factors affecting the tissue elasticity measurement using SWE. The schematic diagram of the phantom constructed is shown in Figure 1.

Construction of Background Phantom

The transparent background phantom mimicking breast fatty tissue was prepared by dissolving 80 g of gelatine powder in 800 ml of boiling deionized water under continuous stirring at 400 rpm for 30 min. The gelatine solution was then poured to a plastic container to form a supportive layer of 2.0 cm and allowed to congeal at room temperature for 8 hours. Spherical inclusions of different gelatine concentrations and diameters were embedded as shown in Figure 1. The gelatine solution was poured over the embedded spherical inclusions, covering both the bottom layer and the spherical inclusions. This process was repeated until all the inclusions were successfully embedded in the congealed gelatine phantom.

Construction of Spherical Inclusions

Spherical inclusions of different stiffness were prepared by mixing different amount of gelatine (8 to 24 g with 4 g interval) and 0.5 g of $CaCO_3$ as scatterer in 150 ml deionized water to mimic the lesions of different elasticities. Industrial food colouring (5% Carmoisine) was added to the spherical inclusions to allow visual differentiation of the spherical inclusions from the transparent phantom background. The spherical inclusions of different diameters, ranging from 1.7 to 3.0 cm, were also prepared to simulate lesions of different sizes. The specifications of each spherical inclusions in the phantom are given in Table 1. Each spherical inclusion was made in pair using the same batch of gelatine mixture and was used for SWE and in vitro electromechanical elasticity measurements (gold standard). Figure 2 shows the gelatine phantom with multiple spherical inclusions embedded in the phantom for SWE measurement.

Elasticity Measurement using SWE

Elasticity of the spherical inclusions was measured using the SWE ultrasound system (Supersonic Imagine, Aix-en-Provence, France). The linear probe (SuperLinear™ SL18-5, Supersonic Imagine, France) was used for B-mode imaging and elastography acquisition at a frequency range of 5 to 18 MHz. The axial and lateral resolutions at -6 dB were 0.3 – 0.5 mm and 0.3 – 0.6 mm, respectively. The linear probe was gently placed (without hard pressing) on the surface with a generous amount of acoustic gel to avoid stiffness radiating from the surface. A good quality B-mode image in term of image brightness was obtained before proceeding with the SWE measurement. During SWE measurement, the Region of Interest (ROI) was placed on the lesion. The elasticity within the ROI was represented by a colour map and was overlaid on the B-mode image (Figure 3). For quantification of elasticity, the "Q-box" as indicated by the circle within the ROI was placed over the tissues of interest. The mean, minimum, maximum and standard deviation of the elasticity along with the diameter of the Q-box were quantified and displayed next to the image (Figure 3). Multiple Q-boxes can be placed within an ROI and the mean elasticity of each spherical inclusion in this study was obtained from four Q-boxes[9,10].

In vitro Tissue Elasticity Measurement

The in vitro elasticity measurement of the spherical inclusions was made using a calibrated Instron electromechanical micro tester system (model 5848, Instron Co, USA). The spherical inclusions were cut into cylindrical shape with a diameter to height ratio of 2:3 to allow uniform stress applied on the surface of the samples and reduce the possibility of stress non-uniformities at sample edges. The compressive test was performed at displacement-control rate of 0.1 mm/min which is equivalent to a strain rate of 0.03/min. The compressive stress (kPa) against strain graph was obtained from the dedicated software in the system. The compressive stress increased exponentially until the elastic limit of the samples achieved and the compression stopped instantly. The Young's modulus of each sample was then estimated from the initial slope of the stress-strain curve in the linear elastic region.

Statistical Analysis

The elasticity of each spherical inclusions measured by the SWE and the Instron electromechanical microtester were compared statistically using paired-sample t-test with 95% confidence level. All statistical analyses were performed using SPSS statistical software (version 24.0, IBM, NY, USA).

Results

Comparison of Elasticity Measured Using SWE and Electromechanical Microtester

Figure 4 shows the elasticity of the spherical inclusions, as measured using SWE and Instron electromechanical microtester (gold standard for elasticity determination). The elasticity was found increased linearly with the increase in the gelatine concentrations (R^2=0.97). The elasticity of the spherical inclusions of different gelatine concentrations (8.5 – 117.6 kPa) measured using Instron electromechanical microtester was found significantly lower ($p<0.05$) than the elasticity obtained using SWE measurements from 16.0 to 125.4 kPa. A mean elasticity difference of 22.8 ± 15.0 kPa was found between the elasticity measured using SWE and Instron electromechanical microtester. The elasticity measurements made by SWE were of overestimation of the actual elasticity by 7 to 39 kPa.

Effect of Size, Stiffness and Depth of Spherical Inclusions on the Elasticity Measurements

The effects of lesion's size and depth from the surface on the SWE elasticity were shown in Figure 5. The SWE elasticity of the spherical inclusions was ranging from 110.3 – 123.2 kPa (Figure 5). The size of the spherical inclusion has no significant effect on the SWE elasticity. The effect of the depth of the spherical inclusions from the surface of the phantom on the elasticity as measured using SWE can be seen from Figure 6. The elasticity of the spherical inclusions at five different depths from the surface of the phantom at 2.7, 4.7, 6.7, 8.7 and 10.7 cm were studied. It should be noted from the figure, the elasticity of the spherical inclusions at 8.7 and 10.7 cm could not be detected by the SWE. Nonetheless, the elasticity of the spherical inclusions at 2.7, 4.7 and 6.7 cm, ranging from 97.5 – 122.6 kPa, does not varied significantly between each other.

Discussion

The tissue-equivalent phantom with human breast tissue acoustic and elastic properties was successfully constructed using water-based gelatine in this study. Although different tissue-equivalent materials are available, the water-based gelatine was selected due to its ability to resembles the stiffness of human breast tissues at 5 – 135 kPa range[11,12]. In addition, the phantom properties such as stiffness, sound speed, absorption and scattering can be independently manipulated by altering the concentration of gelatine and scatterer. Furthermore, gelatine does not exhibit the drawbacks posed by other materials such as copolymer-in-oil and polyacrylamide used in the previous studies[13-15]. The copolymer-in-oil phantom could not achieve the same range of soft tissue acoustic velocities despite showing optimal mechanical properties. Whereas the polyacrylamide gel is known to be fragile and neurotoxic, thus, special precaution during the preparation is needed.

The stiffness of the phantom is dependent on the concentration of the gelatine where a stiffer spherical inclusion will be obtained with higher the gelatine concentration. The gelatine phantom constructed showed a linear correlation between the gelatine concentration and the stiffness of the phantom. The range of the elasticity of the developed phantom at 8.5 – 117.6 kPa covers a wider range of human breast tissues elasticity and even wider than the elasticity range covers by the currently commercially available phantom at 8 – 80 kPa. Although the tissue elasticity measured by SWE was highly correlated with the gold standard, the elasticity obtained using SWE measurements were consistently higher than the elasticity obtained from the Instron micro tester. The overestimation of the elasticity observed can be attributed to two major factors. Firstly, the tissue elasticity computed from SWE measurement was based on the assumption that the density of all tissues in the body equals to 1 g/cm^3. However, there is variation in the density of different human tissues in reality. For example, the density of adipose tissue is ~0.9 g/cm^3 [16] while the density of muscle tissue is ~1.0597 g/cm^3 [17]. In view of this, the dependency of the tissue elasticity as measured using SWE on the actual tissue density would be a suggested area for future research.

Secondly, presence of elasticity boundaries within the phantom media might be responsible for the observed overestimation. The shear wave reflection due to the presence of elasticity boundaries could either induces constructive or destructive interference[18], leading to the underestimation or overestimation of the actual elasticity. Such artefacts can be more complex when multiple elastic reconstructions are combined to form a single elasticity image[19]. A spatio-temporal directional filter, similar to those used in magnetic resonance elastography[20], has been developed to separate the incident and reflect the propagating shear waves. The developed filter has drastically reduced the artefacts in the reconstructed shear modulus map of a stiff inclusion, as well as improved the signal-to-noise ratio of the acquired data[21]. Therefore, it is highly recommended to apply such filter in transient shear wave applications to reduce the reflection artefacts and thus improved the accuracy of tissue elasticity measurement.

Since the elasticity of the spherical inclusions of different diameters and located at different depths from the surface of the phantom are essentially similar, the size and the depth of the lesions have not imposed any effect on the elasticity measurements using SWE. In view of the above, the SWE could be used to for elasticity diagnosis for the lesions up to 3.0 cm. However, the elasticity of the inclusions at the depth greater than 8 cm from the surface could not be assessed using SWE in this study due to the limitation of useful depths for shear wave detection, which were 5 and 8 cm using linear and curvilinear probe, respectively. Therefore, the elasticity for the lesions seeded more than 8 cm from the surface could not be measured.

The phantom constructed in this study can be used for routine quality control to assess the accuracy and reproducibility of elasticity measurements using SWE. The elasticity of the inclusions can be validated using the electromechanical microtester, the gold standard used for elasticity measurement. The preparation of this gelatine phantom is relatively easy as it only involves dissolving the gelatine with heat. Furthermore, the preparation does not involve any hazardous chemical reagents unlike other phantom materials such as PAA. The cost to construct the gelatine phantom are also low looking at the cost of the gelatine, which is only 0.16 USD per gram of gelatine and the estimated cost of the phantom will be lower than 25 USD per phantom. However, since the electromechanical micro tester is a destructive stress-strain measurement tool, therefore, it is advisable to prepare multiple sets of inclusions from the same batch of gelatine mixture for the elasticity measurements using both SWE and electromechanical micro tester.

Conclusion

SWE has provided a better diagnosis outcome by combining the ultrasound images and quantitative tissue elasticity information. Although the SWE has been shown to possess a great potential to improve sensitivity and specificity of breast, liver, thyroid and prostate diseases, however, the accuracy of the elasticity measurement should be validated. Hence, this study described the preparation of a low cost,

reproducible gelatine phantom for the accuracy validation of SWE measurements. In comparison to the gold standard, the elasticity measurement using commercial SWE system has constantly overestimated the elasticity. The elasticity overestimation using SWE can be ascribed to the presence of wave interference at the elasticity boundary. For SWE to be incorporated into clinical diagnostic practice, it is vital to identify a solution to overcome these artefacts.

References

1. Leong SS, Jalalonmuhali M, Md Shah MN, et al. Ultrasound shear wave elastography for the evaluation of renal pathological changes in adult patients. Brit J Radiol. 2023;96(1144):20220288. Doi: https://doi.org/10.1259/bjr.20220288
2. Hirooka M, Koizumi Y, Nakamura Y, et al. Spleen stiffness in patients with chronic liver disease evaluated by 2-D shear wave elastography with ultrasound multiparametric imaging. Hepatology Research.2023;53(2):93-103. Doi: https://doi.org/10.1111/hepr.13841
3. Chen ZT, Jin FS, Guo LH, et al. Value of conventional ultrasound and shear wave elastography in theassessment of muscle mass and function in elderly people with type 2 diabetes. European Radiology. 2023:1-9. Doi: https://doi.org/10.1007/s00330-022- 09382-2
4. Tahmasebi A, Wessner CE, Guglielmo FF, et al. Comparison of Magnetic Resonance-Based Elastography and Ultrasound Shear Wave Elastography in Patients with suspicion of Non-alcoholic Fatty Liver Disease. Ultrasound Quarterly.2023. Doi: 10.1097/ruq.0000000000000638
5. Shiva M, Wei C, Molana H, et al. Cost-Effectiveness of Prostate Cancer Detection in Biopsy-Naïve Men: Ultrasound Shear Wave Elastography *vs*. Multiparametric Diagnostic Magnetic Resonance Imaging. In Healthcare. 2022;10(2):254. Doi: https://doi.org/10.3390/healthcare10020254
6. Cepeha CM, Borlea A, Paul C, et al. Shear-Wave Elastography in Diffuse Thyroid Diseases. Elastography: Applications in Clinical Medicine. 2022:197.
7. Bulum A, Ivanac G, Manduric F, et al. Contribution of UltraFast™ Ultrasound and Shear Wave Elastography in the Imaging of Carotid Artery Disease. Diagnostics. 2022;12(5):1168. Doi: https://doi.org/10.3390/diagnostics12051168
8. Sarvazyan AP, Skovoroda AR, Emelianov SY, et al. Biophysical bases of elasticity imaging. Acoustical imaging.1995:223-40. Doi: 10.1007/978-1-4615-1943-0_23
9. Landberg T, Chavaudra J, Dobbs J, et al. ICRU reports. Reports of the International Commission on Radiation Units and Measurements. 1999;(1):48-51. Doi: https://doi.org/10.1093/jicru_os32.1
10. Kennedy KM, Chin L, McLaughlin RA, et al. Quantitative micro-elastography: imaging of tissue elasticity using compression optical coherence elastography. Scientific reports. 2015;5(1):1-2. DOI: 10.1038/srep15538
11. Orguc S, Acar CR. Correlation of Shear-Wave Elastography and Apparent Diffusion Coefficient Values in Breast Cancer and Their Relationship with the Prognostic Factors. Diagnostics. 2022;12(12):3021. Doi: https://doi.org/10.3390/diagnostics12123021
12. Lee G, Han SB, Lee JH, et al. Cancer mechanobiology: microenvironmental sensing and metastasis. ACS Biomater Sci Eng. 2019;5(8):3735-52. Doi: https://doi.org/10.1021/acsbiomaterials.8b01230
13. Grillo FW, Cabrelli LC, Ribeiro LT, et al. White-silicone rubber and copolymer-in-oil blend for ultrasound soft tissue mimicking material. 2017 IEEE Int. Ultrason.Symp. 2017;Sep 6:1-4. Doi: 10.1109/ULTSYM.2017.8092022
14. Cabrelli LC, Grillo FW, Carneiro AA, et al. Copolymer-in- oil tissue-mimicking material with tunable acoustic properties. In2016 IEEE Int. Ultrason Symp. 2016:1-4. Doi: 10.1109/ULTSYM.2016.7728859
15. Rao SN, Mythravaruni P, Arunachalam K, et al. Mechanical response of polyacrylamide breast tissue phantoms: Formulation, characterization and modeling. J Mech Behav Biomed Mater. 2022;129:105125. Doi: https://doi.org/10.1016/j.jmbbm.2022.105125
16. Vrbaski S, Peña LM, Brombal L, et al. Characterization of breast tissues in density and effective atomic number basis via spectral X-ray computed tomography. arXiv preprint arXiv:2302.06979.2023. Doi: https://doi.org/10.48550/arXiv.2302.06979
17. Ward SR, Lieber RL. Density and hydration of fresh and fixed human skeletal muscle. J Biomech. 2005;38(11):2317-20. Doi: https://doi.org/10.1016/j.jbiomech.2004.10.001
18. Bouchet P, Gennisson JL, Podda A, et al. Artifacts and technical restrictions in 2D shear wave elastography. Ultraschall in der Medizin. Euro Ultraschall Med. 2020;41(03):267-77. Doi: 10.1055/a-0805-1099
19. Pelivanov I, Gao L, Pitre J, et al. Does group velocity always reflect elastic modulus in shear wave elastography?. J Biomed Opt. 2019;24(7):076003. Doi: https://doi.org/10.1117/1.JBO.24.7.076003
20. Manduca A, Bayly PV, Ehman RL, et al. MR elastography: Principles, guidelines, and terminology.Magn Reson Med. 2021;85(5):2377-90. Doi: https://doi.org/10.1002/mrm.28627
21. Mohammed S,Kozlowski P, Salcudean S. Phase-Regulari zed and Displacement-Regularized Compressed Sensing for Fast Magnetic Resonance Elastography. NMR in Biomedicine.2023:e4899.

Doi:https://doi.org/10.1002/nbm.4899

ACKNOWLEDGEMENTS

This work was financially supported by the University of Malaya Postgraduate Research Grant (PO035-2012B). The authors thank the Faculty of Medicine, University of Malaya for providing necessary facilities to carry out this work.

PEER REVIEW

Not commissioned. Externally peer reviewed.

CONFLICTS OF INTEREST

The authors declare that they have no competing interests.

FUNDING

This work was financially supported by the University of Malaya Postgraduate Research Grant (PO035-2012B).

ETHICS COMMITTEE APPROVAL

Medical ethics is not applied in this study since it is a pure phantom study.

Figures and Tables

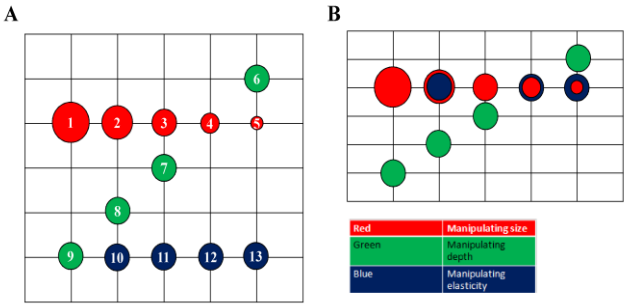

Figure 1: Schematic diagram of the gelatine-based phantom from the top view (A) and side view (B).

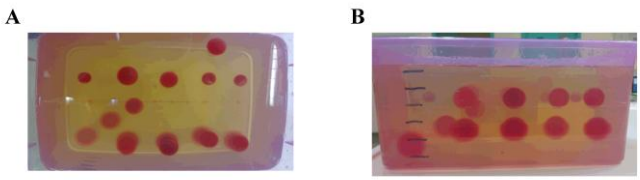

Figure 2: The custom-made SWE phantom for elasticity measurement from top view (A) and side view (B).

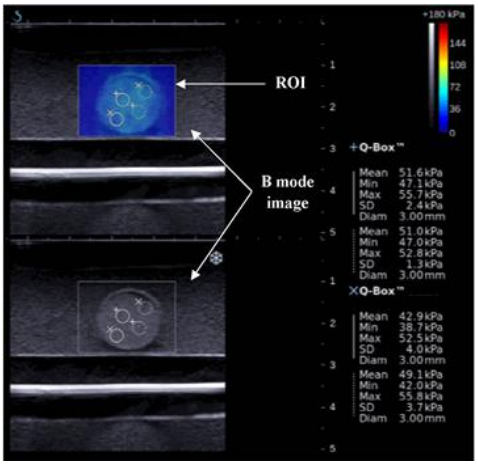

Figure 3: Example of the SWE measurement result displayed on the SWE system. The SWE colour map appeared live on the top half of the display and the bottom half was the image in B-mode. Four Q-boxes were placed over the tissues of interest to measure the tissue elasticity. The colour scale on the top right depicts quantitative values of elasticity shown in the Q-box while the mean, minimum, maximum and standard deviation of the elasticity value as well as the diameter of the Q-box are given in table at the right bottom.

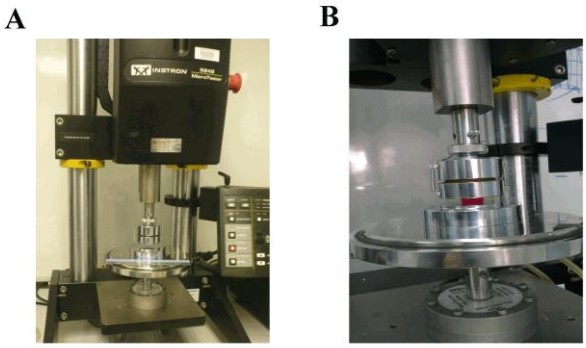

Figure 4: (A) The high precision Instron microtester for in vitro destructive test for soft tissue elasticity measurement. (B) The sample was compressed mechanically by two compression plates at a control rate of 0.1 mm/min.

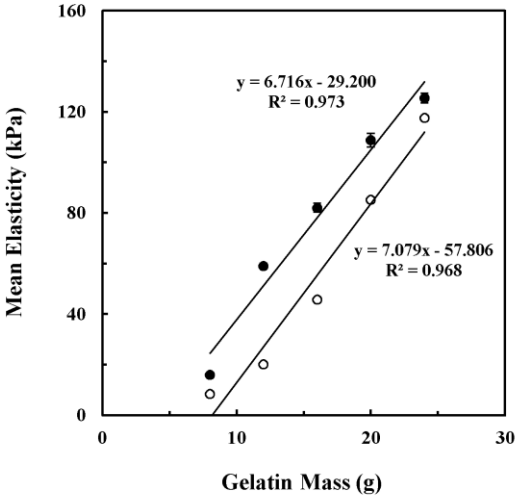

Figure 5: Comparison of elasticity of the spherical inclusions of different gelatine concentrations measured by the SWE (solid circle) and Instron microtester (open circle).

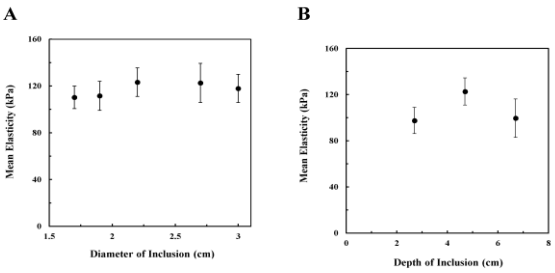

Figure 6: Effects of different diameters (A) and depths from the surface (B) of the spherical inclusions on the elasticity as measured using SWE.

Table 1: Specifications of each inclusion in the phantom.

Studied Factors	Inclusion Number	Diameter (mm)	Depth from Surface (mm)	Gelatine Concentration (g)
Size	1	30	47	16
	2	26	47	16
	3	22	47	16
	4	19	47	16
	5	17	47	16
Depth	6	26	27	16
	7	26	67	16
	8	26	87	16
	9	26	107	16
Elasticity	10	26	47	8
	11	26	47	12
	12	26	47	20
	13	26	47	24

Received: *24-Mar-2023, Manuscript No. AMJ-23-3944;* ***Editor assigned:*** *27-Mar-2023, PreQC No. AMJ-23-3944(PQ);* ***Reviewed:*** *10-Apr-2023, QC No. AMJ-23-3944;* ***Revised:*** *15-Apr-2023, Manuscript No. AMJ-23-3944(R);* ***Published:*** *24-Apr-2023*